

NUMERICAL AND EXPERIMENTAL STUDIES OF TORUS-LIKE FLAME AROUND THE VORTEX FILAMENT IN A PREMIXED REACTANT FLOW

Y. Shoshin*, V.N. Kurdyumov **, L.P.H. de Goey*

vadim.k@ciemat.es

*Department of Mechanical Engineering, Technische Universiteit Eindhoven,
Den Dolech 2, P.O. Box 513, 5600 MB Eindhoven, The Netherlands

** Department of Energy, CIEMAT, Avda. Complutense 40, 28040 Madrid, Spain

Abstract

In this work we present numerical studies and experimental observations of premixed torus-like flames formed around the filament of a steady vortex in a flow of premixed reactants at lean conditions. The numerical results were obtained within the diffusive-thermal model while the experimental observations were carried out for pure methane-air and 50% hydrogen +50% methane-air mixtures. The parallels between such flames and the flame ball are observed owing to delivering of reactants to the curved flame front and removing of combustion products solely by diffusion.

Introduction

The earliest mention of steady flames in a quiescent medium of premixed reactants, later named "flame balls", can be traced back to the article by Drozdov and Zel'dovich [1]. Despite the fact that reactants are initially uniformly mixed, flame balls are essentially diffusion flames: reactants are delivered to the curved flame front, and combustion products are removed solely by diffusion. Though adiabatic flame balls were predicted to be unstable, radiation heat losses could have a stabilizing effect on these flames, see [2]. Later, steady or nearly steady flame balls were experimentally discovered by Ronney [3] at microgravity conditions.

Microgravity flame balls have been observed only in ultra-lean mixtures with a very small Lewis number, and, as later theoretical analysis showed, were indeed stabilized by the radiation heat losses. Due to preferential diffusion effects, the flame temperature of flame balls can largely exceed the adiabatic combustion temperature for the surrounding mixture [2]. The rigorous mathematical derivation of the phenomenon was done in [4, 5]. The flame-ball motion under the action of the free convection generated by itself in the presence of a weak, uniform gravity field was investigated in [6]. Studies of self-drifting flame balls and situations where the gas-velocity components around the flame ball are assumed to be time-dependent were carried out in [7, 8, 9].

"Ideal" flame balls in a quiescent mixture are stretch-less flames as the gas velocity is zero everywhere. The preferential diffusion in such flame balls is, therefore, induced solely by the flame curvature. At the same time, near-uniform steady spherical flames may exist in premixed reactants even in the presence of weak convective flows. Such flames have been observed e.g. in tubes in normal gravity experiments [10] or in counterflow microgravity experiments around the stagnation point [11]. As well as microgravity flame balls,

flame balls in the presence of convection flows were also observed for small Lewis number mixtures. Though the presence of convection may render flame ball locally stretched, the net stretch rate over the whole surface for such flame balls is still zero, which follows the fact that the flame is enclosed and its total surface area does not change with time. This fact suggests that preferential diffusion for flame balls affected by weak convection is also primarily induced by the pure flame curvature, like it takes place for "ideal" flame balls. In the presence of convective flows, radiation losses may become of secondary importance for the flame stabilization as heat can be removed more effectively by the gas convection flow [10].

A 2D analog of flame ball, i.e. infinitely long steady flame tube, can not exist in quiescent medium of premixed reactants: if a constant reaction rate is assumed at the surface of an infinitely long cylinder, an ever growing volume of combustion products and reactants would accumulate with time around the flame [2]. At the same time, the existence of flame tubes which would be physically similar to flame-balls (i.e. ones with zero net flame stretch rate) does not seem impossible when a gas convection at the flame periphery is present, as convection flow could prevent accumulation of heat and combustion products, and depleting of reactants around the flame tube.

Steady flame tubes were found to form at lean limit conditions in small Lewis number mixtures in 2-D premixed counterflow formed by two opposite slit nozzles [12]. Flame tubes were located in the stagnation plane and directed along the (accelerating) gas flow. Similarity of such flame tubes to flame-balls is, however, limited because such flame tubes are stretched not only locally but also globally. Indeed, the gas acceleration along the tube produces the net positive flame stretch rate. Besides, because of gas motion (through the flame tube front) toward the stagnation plane, there is a continuous net gas inflow into the flame tube interior at every cross-section, which does not take place in the case of flame balls. This gas inflow produces an additional positive flame stretch induced by the flame tube curvature.

In this paper, we report the results of numerical simulations and experimental observations of torus-like flames, which otherwise can be considered as enclosed flame tubes. Such flames were observed to form around the filament of a steady vortex in the flow of premixed reactants at very lean conditions. The fully enclosed shape of the observed flames assures that, like in the case of flame-ball like flames, the net flame stretch over the flame surface is zero. Studying such flames can be practically relevant, for example, to investigate flammability limits in the case of the mixture flow in channels with steps or obstacles, near which steady vortices may form. Recently, the flames of this type were investigated numerically behind the trailing edge of a semi-infinite cylindrical rod placed coaxially in a circular channel [13].

Mathematical formulation

The sketch of the numerical problem under consideration is shown in Fig. . Anticipating the description of the experimental setup, the geometrical parameters of the computational domain are chosen in accordance with the experimental conditions described in a pertinent section. A combustible mixture is supplied from a circular porous plug of radius R with a constant wall-normal velocity U_0 . The porous plug and all walls are assumed to be at a constant temperature equal to the temperature T_0 of the incoming mixture. It is

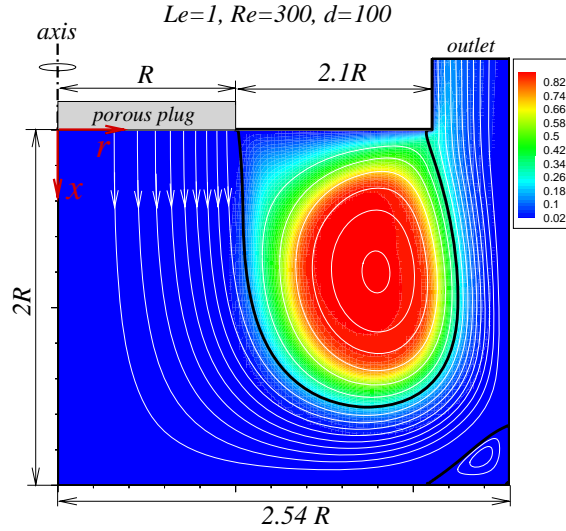


Figure 1: Sketch of the numerical problem, coordinate system, the temperature field (color plot); the isolines of the stream function computed with $Re = 300$, $Le = 1$ and $d = 100$ are plotted with white lines; the thick black lines show the separation values $\psi = 0$ and 0.5 ; the isolines inside the corner recirculation region at the corner $\psi = -0.002$ and -0.004 ; the isolines outside the corner recirculation region at interval of 0.05 .

assumed that all variables remain axisymmetric and the cylindrical coordinate system is employed below.

For the sake of simplicity, the mixture is assumed to be deficient in fuel, so that only its mass fraction denoted by Y with the initial value Y_0 is followed. The mass fraction of the oxidizer, which is in abundance, remains nearly constant. The chemical reaction is modeled by an overall reaction step of the form $F + O \rightarrow P + Q$, where Q is the total heat release, that converts fuel to products at a mass rate proportional to the fuel mass fraction with Arrhenius temperature dependence $\Omega = \mathcal{B}\rho^2 Y \exp(-E/\mathcal{R}T)$, where \mathcal{B} , E and \mathcal{R} are the pre-exponential factor, the activation energy and the universal gas constant respectively.

A diffusive-thermal model is adopted formally assuming that the density of the mixture ρ , the thermal diffusivity \mathcal{D}_T , the individual molecular diffusivity of fuel \mathcal{D} , the heat capacity c_p , and the kinematic viscosity ν are all constant. Consequently, the flow field is not affected by the combustion field and is determined a priori by solving the two-dimensional Navier-Stokes equations.

If the radius of the porous injector R and the wall-normal injection velocity U_0 are chosen as the characteristic length and speed, and the pressure is made dimensionless with respect to the dynamic pressure ρU_0^2 , the velocity field and the pressure satisfy

$$(\mathbf{v} \cdot \nabla)\mathbf{v} = -\nabla p + Re^{-1}\nabla^2\mathbf{v}, \quad \nabla \cdot \mathbf{v} = 0, \quad (1)$$

where $\mathbf{v} = (u_x, u_r)$ is the two-dimensional velocity vector ($u_\varphi \equiv 0$) and $Re = U_0 R/\nu$ is the Reynolds number.

The combustion field is determined by the coupled energy and mass balance equations

with the velocity field computed from (1). In the following, the laminar flame speed of the planar adiabatic flame S_L and the thermal flame thickness defined as $\delta_T = \mathcal{D}_T/S_L$ are used to specify the non-dimensional parameters. The non-dimensional temperature is defined by $\theta = (T - T_0)/(T_e - T_0)$, where $T_e = T_0 + QY_0/c_p$ represents the adiabatic temperature of the planar flame, and the fuel mass fraction is normalized by its upstream value Y_0 . Choosing the convection time R/U_0 as a unit of time, the time-dependent dimensionless transport equations become

$$\frac{\partial \theta}{\partial t} + (\mathbf{v} \cdot \nabla)\theta = \frac{1}{RePr} \Delta \theta + \frac{d}{RePr} \omega, \quad (2)$$

$$\frac{\partial Y}{\partial t} + (\mathbf{v} \cdot \nabla)Y = \frac{1}{LeRePr} \Delta Y - \frac{d}{RePr} \omega, \quad (3)$$

where $\Delta = \partial^2/\partial x^2 + \partial/\partial r^2 + r^{-1}\partial/\partial r$ is the Laplace operator. The dimensionless reaction rate ω takes the form

$$\omega = \frac{\beta^2}{2Le u_p^2} Y \exp \left\{ \frac{\beta(\theta - 1)}{1 + \gamma(\theta - 1)} \right\}. \quad (4)$$

Equations (1)-(3) are solved subject to the following boundary conditions. At the injection surface, $x = 0$ and $0 < r < 1$, the injection velocity, the temperature and the mass fraction flux satisfy

$$u_x = 1, u_r = 0, \theta = 0, Y - Le^{-1}\partial Y/\partial x = 1, \quad (5)$$

where the mass fraction flux is prescribed by means of a Robin-type condition. All solid walls are assumed to be nonslip, impermeable and held at a constant temperature

$$u_x = u_r = \theta = \partial Y/\partial n = 0, \quad (6)$$

where $\partial/\partial n$ denotes the wall-normal derivative. At the outlet boundary we require

$$u_r = \partial u_x/\partial x = \partial \theta/\partial x = \partial Y/\partial x = 0 \quad (7)$$

Apart from the geometric parameters fixed in the simulations, the following non-dimensional parameters appear in the above equations: the Zel'dovich number, $\beta = E(T_e - T_0)/\mathcal{R}T_e^2$, the Lewis number, $Le = \mathcal{D}_T/\mathcal{D}$, the heat release parameter, $\gamma = (T_e - T_0)/T_e$, the Prandtl number, $Pr = \nu/\mathcal{D}_T$, the Reynolds number $Re = M/\pi\rho\nu R$, and the reduced Damköhler number, $d = R^2 S_L^2/\mathcal{D}_T^2$. In the calculations reported below, $\beta = 10$, $\gamma = 0.7$ and $Pr = 0.72$ were assigned.

The factor $u_p = S_L/U_L$ arises in Eq. (4) if the planar flame speed, S_L , is used to define the thermal flame thickness $\delta_T = \mathcal{D}_T/S_L$. Here $U_L = \sqrt{2\rho\mathcal{B}Le\beta^{-2}} \exp(E/2\mathcal{R}T_e)$ is the asymptotic value of laminar flame speed obtained for large activation energy ($\beta \gg 1$). The numerical value of u_p , for a given β and Le , is determined as the eigenvalue of the one-dimensional planar adiabatic flame problem. The numerical values of u_p can be found in [14] as a function of the Lewis number calculated for $\beta = 10$ and $\gamma = 0.7$. In particular, u_p calculated for $Le = 1$ and 0.5 is equal to 0.9420 and 0.9849 , respectively.

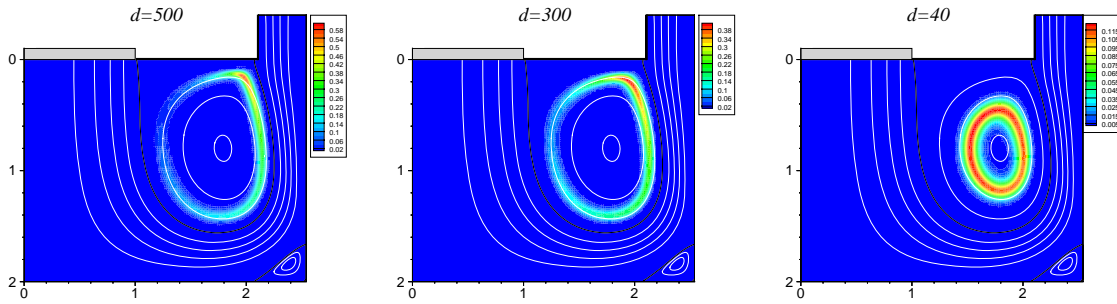


Figure 2: Reaction rate contours (color plot) and the isolines of the stream function computed for several values of d and $Re = 300$, $Le = 1$. The isolines of ψ are at same intervals as in Fig. .

Numerical treatment

A finite-difference second-order, three-point approximation for space derivatives was used in the calculations at a uniform mesh. Equations (1) written in terms of the stream function ψ , defined from the relations $u_x = r^{-1}\partial\psi/\partial r$, $u_r = -r^{-1}\partial\psi/\partial x$, and the vorticity $\zeta = \partial u_r/\partial x - \partial u_x/\partial r$ were solved numerically using a Gauss-Seidel method with over-relaxation.

Steady and unsteady solutions were sought for the reaction-diffusion Eqs. (2)-(3). For the time-dependent calculations, an explicit marching method was used with first-order discretization in time. A sufficiently small time step, dictated by the presence of the highly non-linear chemical reaction term (4), was applied to ensure numerical stability. In order to determine steady (but not necessarily stable) solutions, the marching method was used as well along with the constrain of prescribing the temperature at some reference point; the method is similar to that applied in [15].

Torus-like flames with $Le = 1$

Consider first the case $Le = 1$ simulating in this way lean methane-air mixtures. A typical structure of the flame is illustrated in Fig. where the isotherms and the stream function contours are shown calculated with $Le = 1$, $Re = 300$ and $d = 100$. One can see that the hot temperature region is located completely inside the main vortex in the center of the domain. It is separated from the walls by a cold layer of the fresh mixture. The Moffatt's recirculating eddy located at the corner [16] does not affect the flame structure.

The reaction rate contours are shown in Fig. 2 calculated with $Le = 1$, $Re = 300$ and different d . One can see that the radius of the reaction ring diminishes and it becomes more uniform with decreasing values of the Damköhler number (or, equivalently, decreasing ϕ in experiments).

In order to characterize the flame quantitatively, the maximum of the temperature in the domain, θ_{max} , is used. Figure 3 shows the response curve plotting θ_{max} as a function of the Damköhler number calculated for $Le = 1$ and various Re . All response curves manifest a typical C-shaped behavior illustrated in the inset of Fig. 3.

Of some interest is that the maximum dimensionless temperature θ_{max} increases with

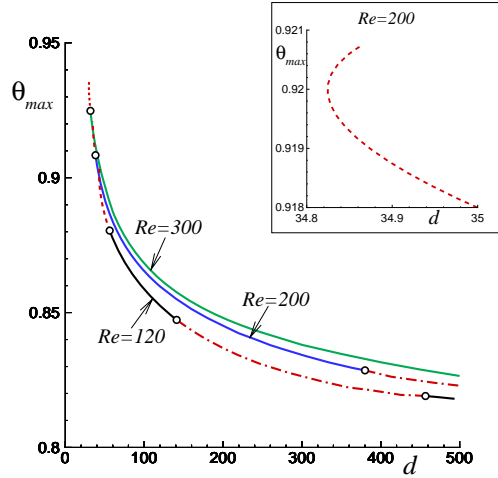


Figure 3: The steady-state maximum temperature as a function of d for several Reynolds number calculated for $Le = 1$: solid segments - stable steady states; dashed segments - unstable steady states (flame extinction); dashed-dotted segments - oscillatory behavior. Open circles indicate the marginal states.

decreasing values of d being below the adiabatic flame temperature and the flame region is becoming relatively hotter. The likely reason is that, with decreasing of d , the flame tube radius diminishes and the flame ring is situated closer to the center of the recirculating region, as seen in Fig. 2. The layer, which separates the flame surface and the edge of the recirculating zone, also thickens. It is important that the flow velocity here is mainly tangential to the flame surface and, then, the heat exchange is dominated by conduction. As a consequence, the heat losses from the flame to the surrounding medium are reduced as the Damköhler number drops.

All curves shown in Fig. 3 represent the steady-state solutions which are not always stable. The time-dependent simulations reveal that the states corresponding to solid segments are indeed stable, for the states plotted with dash-dotted lines an oscillatory behavior develops and the states plotted with dashed lines suffer extinction. In Fig. 4 we illustrate the time histories of the temperature maximum in the domain for distinct d , all curve calculated for $Re = 120$. One can see that for $d = 55$ an oscillatory behavior with increasing amplitude develops leading, finally, to the flame extinction.

It is remarkable that the extinction points have only a weak dependence on the Reynolds number, as seen in Fig. 3. The similar weak dependence was observed also in the experiments reported below. This result can be explained in the following way. At tested mixture flow rates, the convective delivery of the reactants to and removal of the heat and combustion products from the gas layer surrounding the vortex occurs very fast compared to the characteristic diffusion rates inside the vortex. Because of this, the boundary at which temperature and gas composition become equal to the ones in the fresh mixture is always located very close to the surface separating the vortex and the surrounding flow. As a result, heat and mass transport rates are mainly determined by the diffusion process between the flame and the fresh mixture layer in the flow sur-

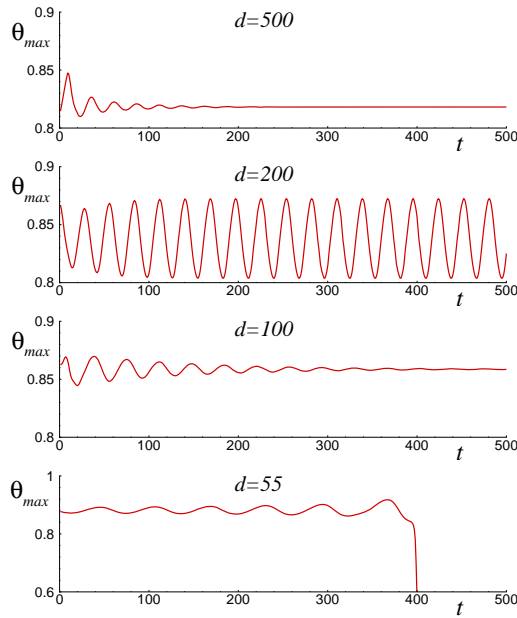


Figure 4: Time history of the maximum temperature in the domain for $Le = 1$, $Re = 120$ and various d . The case $d = 55$ represents the oscillatory behavior with an increasing amplitude and, finally, the flame extinction; the case $d = 200$ exhibits the oscillatory behavior.

rounding the vortex. Because local diffusion fluxes inside the vortex are nearly normal to streamlines, and because the size of the vortex almost does not depend on the mixture flow rate, variations of gas rotation speed practically do not affect characteristic mass and heat diffusion rates inside the vortex and determined by this rates flammability limits.

Torus-like flames with $Le = 0.5$

In order to study the influence of the Lewis number, the simulations have been also performed for $Le = 0.5$ mixture. Figure 5 shows the temperature (upper plot) and reaction rate (lower plot) contours associated with the steady-state solutions obtained for $Le = 0.5$, $Re = 300$ and $d = 0.08$. The distributions are qualitatively similar to those shown in Fig. and 2. The main distinction which can be pointed out is that the temperature maximum exceeds the adiabatic flame temperature. Undoubtedly it occurs due to the preferential diffusion effects, like it takes place for flame balls [2].

Figure 6 shows the maximum temperature θ_{max} plotted versus the Damköhler number calculated for the steady-state solutions with $Le = 0.5$ and various Reynolds numbers. One can see that the maximum temperature significantly exceeds the adiabatic flame temperature also growing with decreasing values of d . All curves also show the well-defined C-shape form where the solid parts of the curves were found to correspond to stable states while the dashed parts were found to correspond to unstable states.

The time-dependent numerical simulations of states shown Fig. 5 are illustrated in Fig. 7. One can see that similar to the $Le = 1$ case, there exists a critical value of d (marked with open circles) below which the steady solution becomes unstably leading

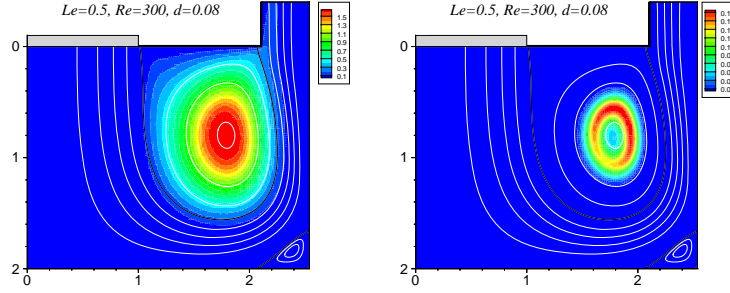


Figure 5: Temperature (a), reaction rate (b) contours and the isolines of the stream function computed for $Le = 0.5$, $Re = 300$ and $d = 0.08$. The isolines of ψ at same intervals as in Figs. and 2.

to the extinction, see the curve with $d = 0.07$. Nevertheless, no oscillatory behavior was observed for $Le = 0.5$.

Experimental observations

Figure 8 shows a schematic of the experimental setup. The flame was stabilized inside a vortex chamber formed by two separate parts. The bottom part of the chamber is represented by a 25 mm long and 25.4 mm ID fused silica cup. The top part consists of 22 mm OD cylindrical brass cup with a flat 2 mm thick perforated bottom (0.5 mm holes, arranged in a hexagonal pattern with a 0.7 mm pitch) and a 10 mm ID 20 cm long brass tube centered inside the brass cup and attached to the brass cup bottom from inside. The mixture was supplied through the tube and entered the vortex chamber through the central 10 mm diameter part of the perforated bottom, while the rest of perforation was blocked. The fused silica cup was mounted on a vertical positioner, allowing the adjustment of the vortex chamber height, i.e. the spacing between the fused silica plate and the bottom of the brass cylinder. The experiments reported in this paper were performed at a fixed camera height of 10 mm. To ignite the flame, the fused silica cup was moved downward, leaving 2 cm gap between the fused silica tube edge and the top part of the chamber. An equivalence ratio sufficient for the reliable ignition was set initially and the mixture was ignited below the perforated plate. After that, the fused silica cup was lifted back to form a vortex chamber and equivalence ratio was then step-wise decreased.

Pure methane and 50% hydrogen +50% methane (by volume) mixtures were used as fuel gases. The methane, hydrogen, and air flows were set by mass flow controllers, controlled by a computer with an external DAQ system, which provided communication between the computer and mass-flow controllers. The flame was filmed with a Pike F-032B camera connected to a computer. The camera could be moved between the two fixed positions, one position for filming the side view and another - for the bottom view of the flame (using a first surface mirror installed at 45°).

Experiments have been carried out at mixture flow-rates ranging from 250 to 830

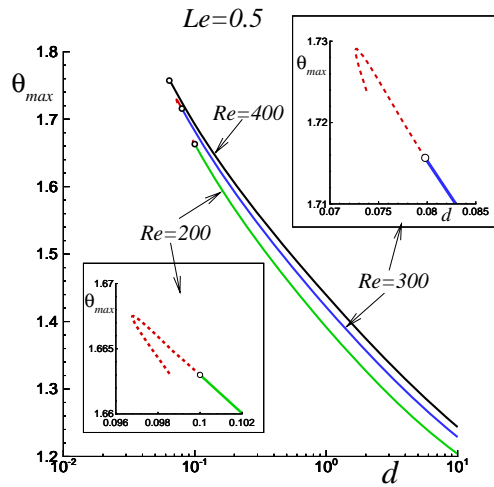


Figure 6: The steady-state maximum temperature as a function of d for several Reynolds numbers calculated for $Le = 0.5$; $\theta = 1$ corresponds to adiabatic flame temperature; solid segments - stable steady states; dashed segments - unstable steady states (flame extinction).

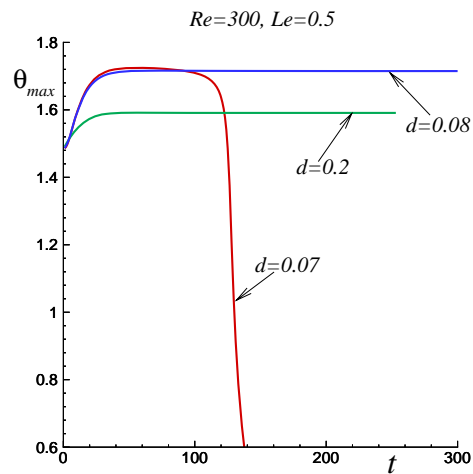


Figure 7: Time history of the maximum temperature in the domain for $Le = 0.5$, $Re = 300$ and various d .

cm^3/s . Similar combustion behavior has been observed for methane-air and (0.5H₂ + 0.5CH₄)-air flames. After the flame had been ignited and the fused silica cup lifted to form a 10 mm tall combustion chamber, the flame escaped with the upward flow through the coaxial slit between the fused silica and brass caps. As, after that, the equivalence ratio was eventually decreased down to near-limit values, the flame became completely localized inside the chamber and enclosed upon itself, taking a torus-like shape. Stable toroidal flames were established at flow rates between 330 and 830 cm^3/s , for mixtures of both methane and (0.5H₂ + 0.5CH₄) fuel gases with air.

Figure 9 shows photographs (side and bottom views) of methane-air and hydrogen-

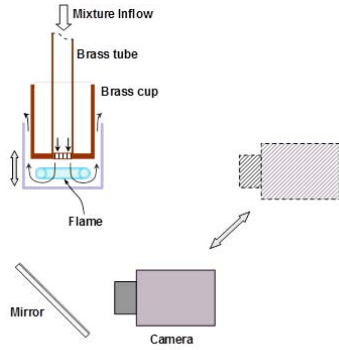


Figure 8: Schematic of the experimental setup.

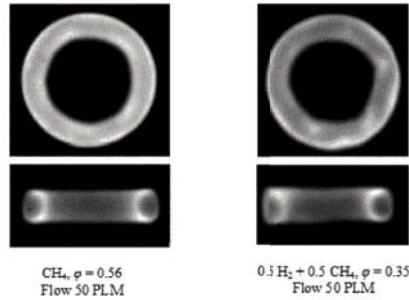


Figure 9: Bottom and side views of toroidal flames of methane-air (left) and hydrogen-methane-air (right) mixtures.

methane-air flames stabilized at a mixture flow rate of $830 \text{ cm}^3/\text{s}$. The equivalence ratio is $\phi = 0.56$ for the methane-air mixture ($Le \approx 0.98$) and $\phi = 0.35$ for the $(0.5\text{H}_2 + 0.5\text{CH}_4)$ -air mixture ("effective" Le , estimated by different formulae suggested in literature ranges from 0.46 to 0.63). Decreasing the equivalence ratio in the experiments leads to a decrease of the torus tube diameter, and then to flame extinction. The equivalence ratios at the lean flammability limit were nearly independent on the mixture flow rate, within the tested range both for plane methane-air and hydrogen-methane air mixtures. At the mixture flow rates of 250 and $830 \text{ cm}^3/\text{s}$, the limit values of the equivalence ratio were found to be, correspondingly, in the range between $\phi = 0.535$ and 0.54 for methane, and between $\phi = 0.30$ and 0.31 for hydrogen-methane flames. Note that flammability limits observed in hydrogen-methane-air mixtures are far below the theoretical limit for the planar zero-stretch flame [17], suggesting that the flame in this $Le < 1$ mixture survives due to the preferential diffusion effects. Because the flame has zero net stretch rate, the preferential diffusion in this case, as in the case of flame balls, is likely to be a pure flame curvature effect.

It is seen on the flame bottom views, Fig. 9, that flame shapes deviate from a perfect torus. At the inner side the methane-air flame looks slightly corrugated, this effect being more prominent for the hydrogen-methane-air flame. It can be speculated, however, that this corrugation is rather a result of the experimental setup imperfection, instead of the intrinsic flame instability. As seen in Fig. 2, the inner edge of the flame has a near-hexagonal shape. Close examination of flame photographs shows that the sides of the "hexagon" are always nearly parallel to the rows of holes in the cylindrical cup button,

which, as mentioned above, are also arranged in an hexagonal pattern. This observation suggests that the flame corrugation occurs due to small non-uniformities of the mixture inlet flow along its periphery, and that flames with of perfect rotationally-symmetric shape could be produced if this flow was perfectly uniform.

Concluding remarks

In this study, we have presented the results of numerical simulations of torus-like premixed flames. This kind of flames appears around the vortex filament in a premixed reactant flow. It should underline a certain analogy between the torus-like flame and the flame ball. In both cases, the reactants are delivered to the flame surface solely by diffusion. The numerical simulations reveal that the maximum temperature inside the torus-like flame increases with decreasing values of the Damköhler number. For the case of the unity Lewis number an interval of d exists where the flame suffers an oscillatory behavior. It does not take place for flames with $Le = 0.5$.

Results of simulations are consistent with experimental observations carried for out for plain methane-air and 50% hydrogen +50% methane-air mixtures. Steady enclosed torus-like flames with near uniform flame fronts are observed in both simulations and experiments. Flammability limits are nearly insensitive to the mixture flow rate (Reynolds number) for experimental and simulated flames.

Acknowledgment

The financial support of the Dutch Technology Foundation (STW), Project 13549, is gratefully acknowledged. V.K. acknowledges also the support of Spanish MEC under project ENE2015-65852-C2-2-R.

References

- [1] Drozdov, N.P., Zel'dovich, Ya. B., "Difusionnie yavlenia u predelov rasprostraneniya plameni. Eksperimental'nie issledovaniya flegmatizatsii bzhivchatih smesei okisoi ugleroda", *Zhurnal Fizicheskoi Khimii (Russian Journal of Physical Chemistry A)* 17(3): 134-144 (1943).
- [2] Zel'dovich, Ya.B., Barenblatt, G.I., Librovich, V.B., Mahkviladze, G.M., *The Mathematical Theory of Combustion and Explosions*, Consultants Bureay, New York, 1985.
- [3] Ronney, R., "Near-Limit Flame Structures at Low Lewis Number", *Combust. Flame* 82: 1-14 (1990).
- [4] Buckmaster, J., Joulin, G., Ronney, P., "The Structure and Stability of Nonadiabatic Flame Ball", *Combust. Flame* 79: 381-392 (1990).
- [5] Buckmaster, J., Joulin, G., Ronney, P., "The Structure and Stability of Nonadiabatic Flame Balls: II. Effects of Far-Field Losses", *Combust. Flame* 84: 411-422 (1991).
- [6] Joulin, G., Kurdyumov, V.N., Liñan, A., "Existence conditions and drift velocities of adiabatic flame-balls in weak gravity fields", *Combust. Theory Modell.* 3: 281-296 (1999).

- [7] Minaev, S.S., Kagan, L., Joulin, G., Sivashinsky, G., "On self-drifting flame balls", *Combust. Theory Modell.* 5: 609622 (2001).
- [8] Minaev, S.S., Kagan, L., Sivashinsky, G., "Self-Propagation of a Combustion Spot in Premixed Gases", *Combust. Explos. Shock Waves* 38(1): 9-18 (2002).
- [9] Joulin, G., Cambray, P., Jaouen, N., "On the response of a flame ball to oscillating velocity gradients", *Combust. Theory Modell.* 6: 5378 (2002).
- [10] Shoshin, Y.L., van Oijen, J.A., Sepman, A.V., de Goey, L.P.H., "Experimental and computational study of the transition to the flame ball regime at normal gravity", *Proc. Combust. Inst.* 33: 1211-1218 (2011).
- [11] Takasea, K., Li, X., Nakamura, H., Tezuka, T., Hasegawa, S., Katsuta, M., Kikuchi, M., Maruta, K., "Extinction characteristics of CH₄/O₂/Xe radiative counterflow planar premixed flames and their transition to ball-like flames", *Combust. Flame* 160 1235-1241 (2013).
- [12] Kaiser, C., Liu, J.B., Ronney, P., "Diffusive-thermal instability of counterflow flames at low Lewis number", *AIAA Paper No 2000-0576*, 38th AIAA Aerospace Sciences Meeting, (Reno, NV, January 11-14).
- [13] Kurdyumov, V.N., Shoshin, Y., de Goey, L.P.H., "Structure and stability of premixed flames stabilized behind the trailing edge of a cylindrical rod at low Lewis numbers", *Proc. Combust. Inst.* 35: 981-988 (2015)
- [14] Kurdyumov, V.N., "Lewis number effect on the propagation of premixed flames in narrow adiabatic channels: Symmetric and non-symmetric flames and their linear stability analysis", *Combust. Flame* 158: 1307-1317 (2011)
- [15] Kurdyumov, V.N., Matalon, M., "Dynamics of an edge-flame in the corner region of two mutually perpendicular streams", *Proc. Combust. Inst.* 31: 929-938 (2007).
- [16] Moffat, H.K., "Viscous and resistive eddies near a sharp corner", *J. Fluid Mech.* 18: 1-18 (1964).
- [17] Van den Schoor, F., Hermanns, R.T.E., van Oijen, J.A., Verplaetsen, F., de Goey, L.P.H., "Comparison and evaluation of methods for the determination of flammability limits applied to methane/hydrogen/air mixtures", *J. Hazard. Mater.* 150: 573-581 (2008).